Available online at www.sciencedirect.com

SciVerse ScienceDirect

Ceramics International 38 (2012) 1187–1193

CERAMICS INTERNATIONAL

www.elsevier.com/locate/ceramint

Phase formation of $REBa_2Cu_3O_{7-\delta}$ (RE: $Y_{0.5}Gd_{0.5}$, $Y_{0.5}Nd_{0.5}$, $Nd_{0.5}Gd_{0.5}$) superconductors from nanopowders synthesised via co-precipitation

M.H. Wahid [a], Z. Zainal [a,b,*], I. Hamadneh [c], K.B. Tan [a], S.A. Halim [d], A.M. Rosli [a,b], E.S. Alaghbari [a], M.F. Nazarudin [a], E.F. Kadri [a]

[a] Department of Chemistry, Faculty of Science, Universiti Putra Malaysia, 43400 UPM Serdang, Selangor, Malaysia
[b] Institute of Advanced Technology (ITMA), Universiti Putra Malaysia, 43400 UPM Serdang, Selangor, Malaysia
[c] Department of Chemistry, Faculty of Science, University of Jordan, 11942 Amman, Jordan
[d] Department of Physics, Faculty of Science, Universiti Putra Malaysia, 43400 UPM Serdang, Selangor, Malaysia

Received 4 August 2011; accepted 23 August 2011
Available online 2 September 2011

Abstract

Phase formation of $REBa_2Cu_3O_{7-\delta}$ (RE: $Y_{0.5}Gd_{0.5}$, $Y_{0.5}Nd_{0.5}$, $Nd_{0.5}Gd_{0.5}$) superconductors synthesised via co-precipitation (COP) method were investigated by thermogravimetric analysis (TGA), differential thermal analysis (DTA) and X-ray diffraction (XRD) analysis. All samples showed identical thermal decomposition behaviour from the thermogram in which 5 major weight losses were observed. However, XRD of the samples at different heat treatment temperatures showed different diffraction patterns indicating different thermolytic processes. Meanwhile, transmission electron microscopy and surface area analysis revealed that the powders obtained from COP have particle sizes ranging from 7 to 12 nm with relatively large surface area. Molar ratios of prepared samples obtained were near to the theoretical values as confirmed by elemental analyses using X-ray fluorescence (XRF). The $T_{C(R=0)}$ for sintered YGd, YNd and NdGd were 87 K, 86 K and 90 K, respectively. Surface morphological study via scanning electron microscope showed the structures of samples were dense and non porous.

Keywords: Oxide; Superconductor; Powders: chemical preparation; Chemical properties

1. Introduction

Recently, preparation of high temperature superconductors via the wet chemical technique has been proven to produce good quality materials with comparable properties to the samples synthesised via solid state method [1–4]. In wet chemistry technique, the initial mixture of cations at atomic scale is allowed thus enhancing the chemical reactions to form desirable phases [2]. This is experimentally proven in which the heat treatment duration has been significantly reduced and the required intermittent grindings becomes unnecessary [1–4]. Formation of superconductor from metal oxalate precursors involves several chemical reactions such as dehydration, oxidation and further reactions with other metal oxides to form binary or ternary compounds. In considering preparation of a complex compound, phase formation study is a prerequisite in order to obtain phase pure samples with optimum properties [5]. This also helps to determine appropriate heat treatment condition.

Various types of high temperature superconductors have been studied since their discovery in 1986 [6] particularly in $REBa_2Cu_3O_{7-\delta}$ or so called RE123 superconductors [7]. This type of superconductor receives huge attention due to their fascinating properties, e.g. relatively high T_C, high J_C and excellent capabilities of trapping magnetic fields [8–10]. There appears a great possibility to substitute isovalent metal ions or other elements with similar ionic radii into either, RE^{3+}, Ba^{2+} or Cu^{2+}/Cu^{3+} sites. However, attempts to enhance the electrical properties by chemical doping require careful understanding in structural change in which the conduction mechanism is influenced. For instance, a number of researchers have reported that $NdBa_2Cu_3O_{7-\delta}$, $GdBa_2Cu_3O_{7-\delta}$ and $SmBa_2Cu_3O_{7-\delta}$

* Corresponding author. Tel.: +60 3 89486101x3509; fax: +60 3 89432508.
E-mail address: zulkar@putra.upm.edu.my (Z. Zainal).

0272-8842/$36.00
doi:10.1016/j.ceramint.2011.08.048

exhibit superior properties such as higher T_C and J_C if compared to the typical $YBa_2Cu_3O_{7-\delta}$ [8–12].

In this study, the prepared materials namely $REBa_2Cu_3O_{7-\delta}$ (RE = $Y_{0.5}Nd_{0.5}$, $Y_{0.5}Gd_{0.5}$ and $Nd_{0.5}Gd_{0.5}$) are of particular interest in which it has been reported that by mixing trivalent rare earth element, materials with higher T_C and J_C was obtained [13–16]. It is therefore we report the formation study and physicochemical properties of these mixed RE superconductors.

2. Experimental

2.1. Preparation of $REBa_2Cu_3O_{7-\delta}$ ceramic oxides

$REBa_2Cu_3O_{7-\delta}$ (RE = $Y_{0.5}Nd_{0.5}$, $Y_{0.5}Gd_{0.5}$ and $Nd_{0.5}Gd_{0.5}$) were synthesised by reagent grade metal acetates of RE (III) acetate [$RE(OOCCH_3)_3{\cdot}xH_2O$; RE = Y, Nd and Gd], barium acetate and copper (II) acetate (purity >99%, reagent grades). The metal acetates were dissolved in acetic acid, namely solution A. Meanwhile, solution B containing 0.5 M oxalic acid was prepared in a mixture of water: isopropanol (v/v = 1:1.5). Solution B was added drop-wise into solution A in an ice bath with continuous stirring. A uniform, stable, blue suspension was formed and the slurry was filtered after 5 min of reaction. This was followed by a drying at 80 °C overnight. The dried blue precipitates were ground prior to thermal treatment at 860 °C in air for 12 h. The calcined powders were reground in an agate mortar for 10 min and cold pressed uniaxially into pellet of 13 mm diameter using Specac manually operated hydraulic press. The pellets were sintered in oxygen atmosphere at 970 °C for 15 h and cooled slowly to room temperature in furnace at a rate 1 °C/min.

2.2. Characterisation

The thermal properties of the metal oxalate precursor powders were analysed by Mettler Toledo TGA/SDTA 851 and Perkin Elmer DTA 7 from 30 °C to 1000 °C at a heating rate of 10 °C/min in air atmosphere. The phase purity of powdered samples was analysed by X-ray powder diffractometer, Shimadzu XRD-6000 with Cu K_α radiation with a step size of 0.02° over the 2θ range 2–60°. Particle size and surface area were investigated via transmission electron microscope (TEM) Hitachi H-7100 and volumetric sorption analyser Quantachrome, Autosorb-1 using N_2 as adsorbent. Elemental analyses were carried out using Shimadzu energy dispersive X-ray fluorescence (XRF) spectrometer. Electrical properties of the pellets were determined by four point probe method using constant current of 30 mA (DC) in the temperature range of 50–300 K. The cryogenic set up is based on the Closed Cycle Helium Cryostat Austin Scientific M125. Surface morphology of the fractured samples was investigated using scanning electron microscopy (SEM) JEOL 6400.

3. Results and discussion

3.1. Physical properties of co-precipitated $REBa_2Cu_3O_{7-\delta}$ (RE = $Y_{0.5}Nd_{0.5}$, $Y_{0.5}Gd_{0.5}$ and $Nd_{0.5}Gd_{0.5}$) metal oxalate precursor powders

XRD analyses of co-precipitated $REBa_2Cu_3O_{7-\delta}$ (RE = $Y_{0.5}Nd_{0.5}$, $Y_{0.5}Gd_{0.5}$ and $Nd_{0.5}Gd_{0.5}$) metal oxalate precursor powders show that all samples have almost similar diffraction patterns (Fig. 1).

Major peaks are found to match with the barium oxalate dihydrate (ICDD: 21-1529) and copper oxalate hydrate (ICDD: 21-0297) phases. Meanwhile, the main peaks of rare earth oxalates could possibly overlap with the barium oxalate dihydrate peaks due to close proximity of their 2θ values. For instance, yttrium, gadolinium and neodymium oxalate hydrate phases have their diffraction plane with highest intensity at 2θ = 13.3–13.6° (ICDD: 33-1460, 20-0411 and 20-0764, respectively). The remaining unidentified peaks are believed to be the combination of co-precipitated phases containing rare earth, barium and copper oxalates [17].

Meanwhile, TEM analysis of co-precipitated powders shows images of agglomerated particles with clearly visible grain boundaries (Fig. 2a–c). The particle sizes of the co-precipitated powders obtained from TEM are in the range of 7–12 nm. On the other hand, the surface area of co-precipitated powders was determined via BET method. BET analysis indicates that these samples have considerably high surface area with values of 24.59, 31.31 and 21.64 m^2/g for $Y_{0.5}Gd_{0.5}Ba_2Cu_3O_{7-\delta}$, $Y_{0.5}Nd_{0.5}Ba_2Cu_3O_{7-\delta}$ and $Nd_{0.5}Gd_{0.5}Ba_2Cu_3O_{7-\delta}$, respectively. The large surface area denotes that the precursor powders are ultra fine and reactive. This is agreeable with TEM results in which very fine particles in nano-meter size are discovered.

3.2. Phase formation of $REBa_2Cu_3O_{7-\delta}$ (RE = $Y_{0.5}Nd_{0.5}$, $Y_{0.5}Gd_{0.5}$ and $Nd_{0.5}Gd_{0.5}$)

The study of phase formation mechanism in such complex reacting mixtures is important for optimisation of the sample

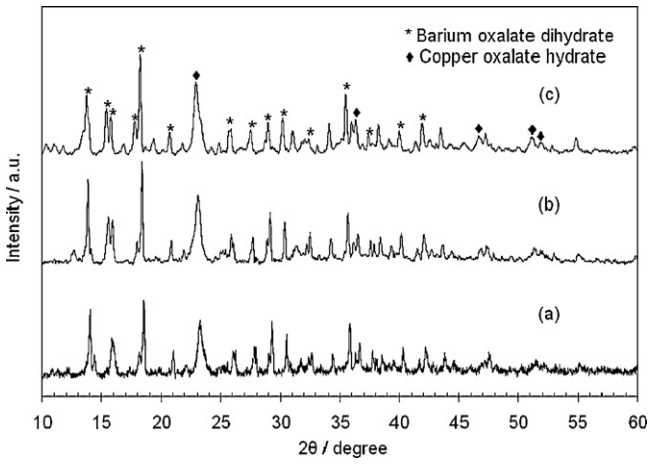

Fig. 1. X-ray diffractograms of co-precipitated (a)YGdBCO, (b)YNdBCO and (c)NdGdBCO metal oxalate precursors.

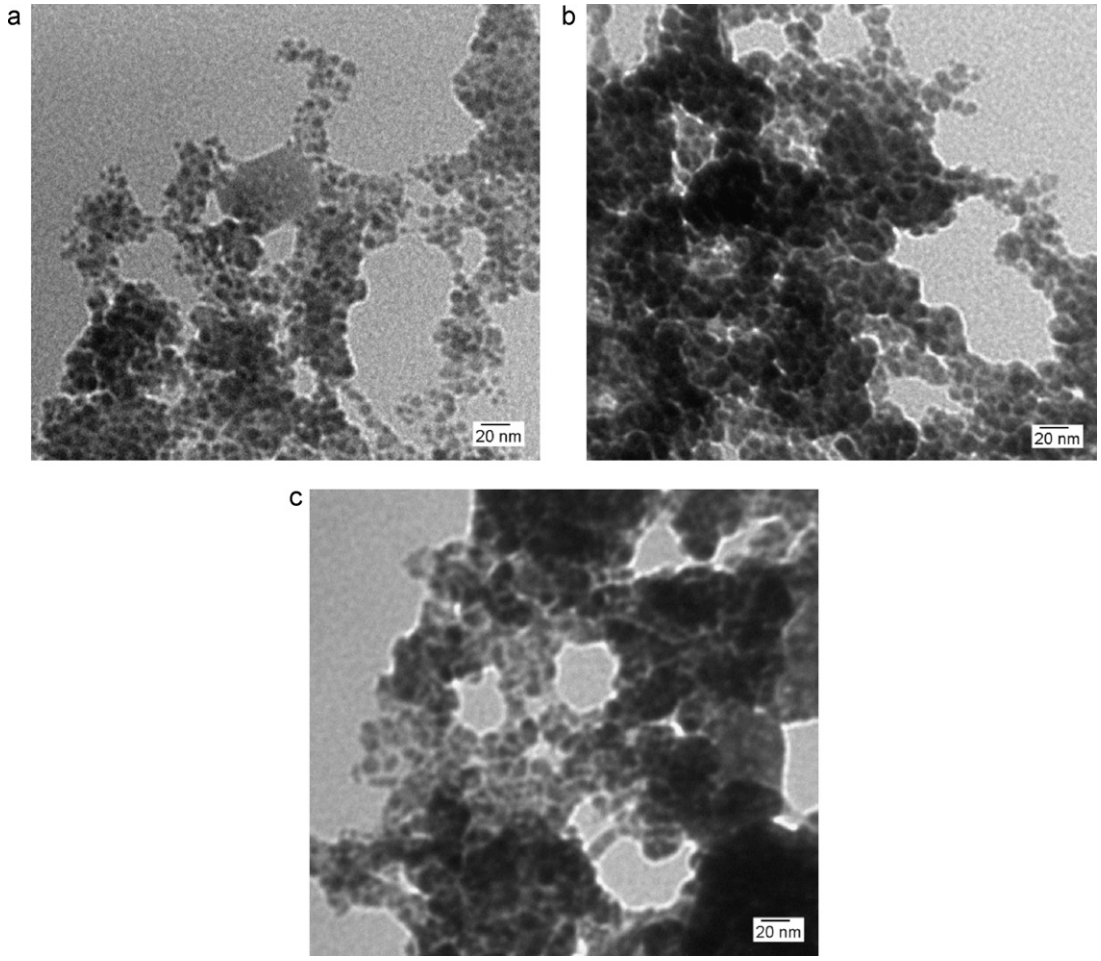

Fig. 2. TEM images of co-precipitated (a)YGdBCO, (b)YNdBCO and (c)NdGdBCO metal oxalate precursors.

preparation, whereby formation of undesirable phases should be suppressed. Moreover, reaction of a complex mixture of powders might lead to formation of many different phases [5], which may affect the properties. In this study, the thermal decomposition behaviour of $REBa_2Cu_3O_{7-\delta}$ (RE = $Y_{0.5}Nd_{0.5}$, $Y_{0.5}Gd_{0.5}$ and $Nd_{0.5}Gd_{0.5}$) metal oxalate precursors are studied via TGA, DTA and XRD analyses.

According to TGA results, all samples display identical thermograms where five major thermal events are discernible (Fig. 3). The weight losses are labelled as drop 1, drop 2, drop 3, drop 4 and drop 5.

For all samples, approximately 18% of weight loss (drop 1 and drop 2) is attributed to the dehydration of moisture and water in crystalline solids, in which the dehydrated RE

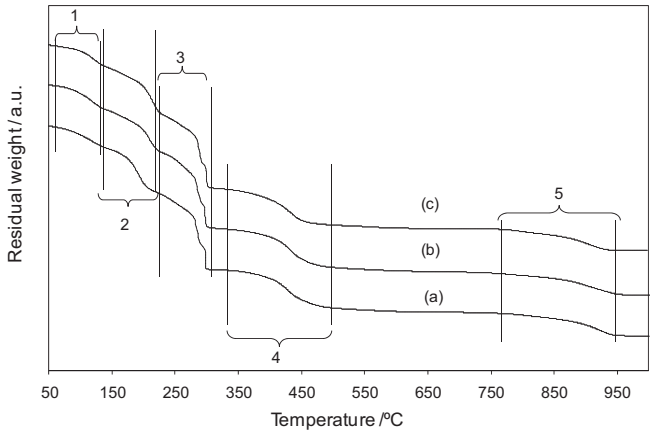

Fig. 3. TGA thermograms of co-precipitated (a)YGdBCO, (b)YNdBCO and (c)NdGdBCO metal oxalate precursors.

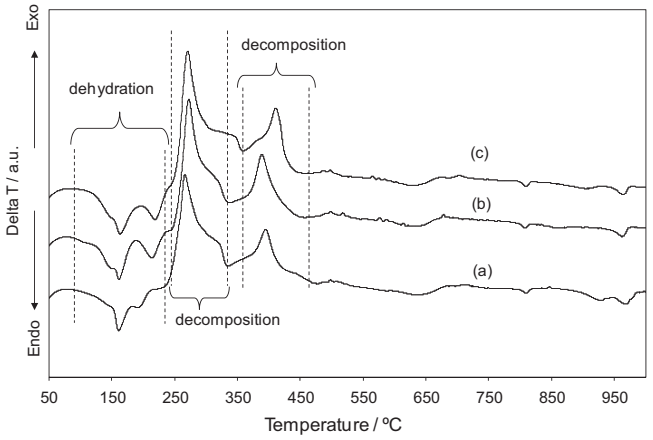

Fig. 4. DTA thermograms of co-precipitated (a)YGdBCO, (b)YNdBCO and (c)NdGdBCO metal oxalate precursors.

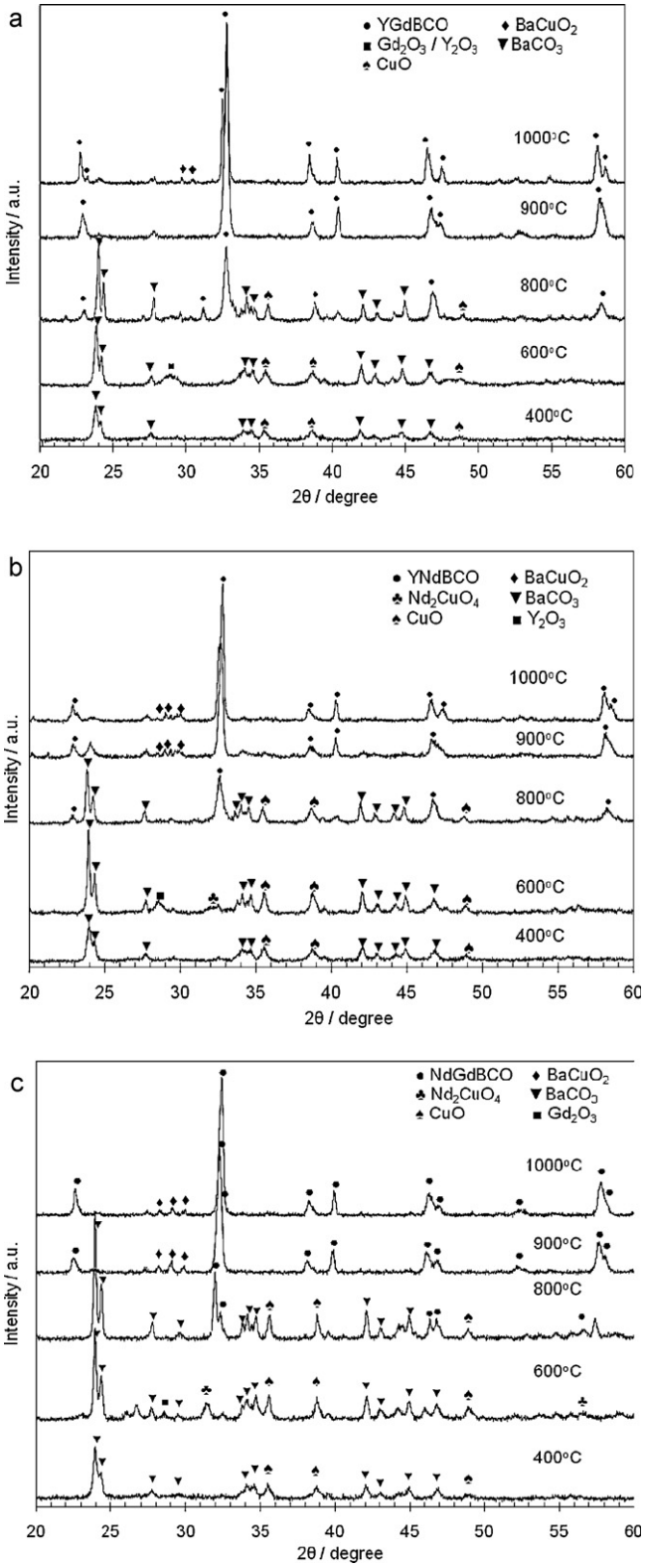

Fig. 5. XRD patterns of prepared samples at different heating temperatures (a)YGdBCO, (b)YNdBCO and (c)NdGdBCO metal oxalate precursors.

oxalates, BaC_2O_4 and CuC_2O_4 are formed. This dehydration process is also confirmed by DTA results where endothermic peaks in the same temperature range could be clearly observed (Fig. 4).

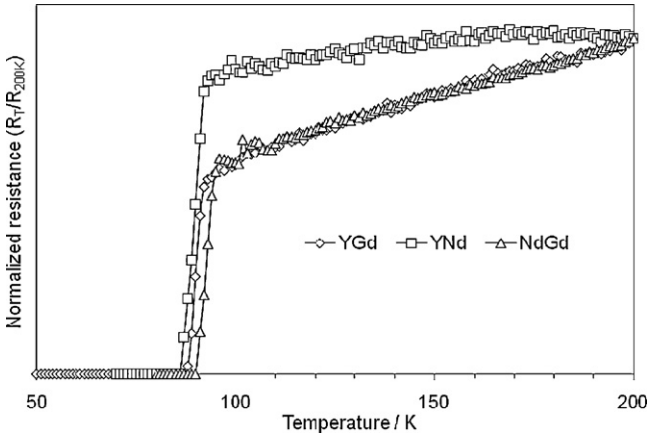

Fig. 6. Electrical resistance of samples obtained after sintering at 970 °C/15 h in oxygen atmosphere.

On the other hand, a sharp weight loss is observed in drop 3 (~200–300 °C) as the dehydrated RE oxalate and copper oxalate starts to transform into RE carbonates and copper oxide respectively. It is a noteworthy to point out that rare earth carbonates are amorphous and therefore they are difficult to be detected by XRD analysis (Fig. 5a–c) [18]. The decomposition process is also complemented by DTA results in which a significant exothermic peak associated to decomposition is observed. Interestingly, similar TGA curves obtained for all three samples show different X-ray diffraction patterns under same heat treatment. This indicates that the thermolytic processes for these samples are different.

For instance, at drop 4 (~300–500 °C), samples containing yttrium and gadolinium which was fired at 600 °C show formation of yttrium oxide (Fig. 5a and b) and gadolinium oxide (Fig. 5a and c) in their XRD results (ICDD: 41-1105, 12-0797, respectively). Meanwhile, decomposition of barium oxalate into barium carbonate is observed after firing at 400 °C (ICDD: 5-0378). Surprisingly, neodymium oxide phase is not formed in neodymium oxalate samples. This leads to formation of Nd_2CuO_4 phase (ICDD: 24-0777) due to the reactive behaviour of Nd at 600 °C. The low activation barrier between Nd and copper oxide allows the reaction to occur at even lower temperature [19].

The mixed ternary ceramic oxides, $REBa_2Cu_3O_{7-\delta}$ are finally completed with the reactions of metal oxides or binary neodymium–copper oxide with barium carbonate at temperature ranging from ~860 to 940 °C. All chemical reactions involved are summarized in Tables 1–3.

3.3. Elemental analysis

Elemental analysis of selected samples sintered at 970 °C/15 h was carried out via X-ray fluorescence (XRF) analysis. The experimental composition of $Y_{0.5}Gd_{0.5}Ba_2Cu_3O_{7-\delta}$ is in good agreement with that calculated theoretically (Table 4). This confirms that stoichiometric $Y_{0.5}Gd_{0.5}Ba_2Cu_3O_{7-\delta}$ is successfully prepared without any significant Cu loss. Meanwhile, comparable results are also observed in other compositions (Table 5).

Table 1
Chemical reactions involved in the formation of $Y_{0.5}Gd_{0.5}Ba_2Cu_3O_{7-\delta}$.

Drop	Weight loss (Δm) (mg)	Δm (experimental) (%)	Δm (theory) (%)	Temperature range (°C)	Reaction
1–2	3.27	16.21	16.21	41–219	Water loss from the sample
3	3.86	19.13	19.91	219–309	$3Cu(C_2O_4) + (3/2)O_2 \rightarrow 3CuCO_3 + 3CO_2$ $3CuCO_3 \rightarrow 3CuO + 3CO_2$ $(1/4)Y_2(C_2O_4)3 + (3/8)O_2 \rightarrow (1/4)Y_2(CO_3)_3 + (3/4)CO_2$ $(1/4)Gd_2(C_2O_4)3 + (3/8)O_2 \rightarrow (1/4)Gd_2(C\ O_3) + (3/4)CO_2$
4	1.94	9.62	9.42	310–520	$2Ba(C_2O_4) + O_2 \rightarrow 2BaCO_3 + 2CO_2$ $(1/4)Y_2(CO_3)_3 \rightarrow (1/4)Y_2O_3 + (3/4)CO_2$ $(1/4)Gd_2(CO_3)_3 \rightarrow (1/4)Gd_2O_3 + (3/4)CO_2$
5	1.14	5.64	6.79	741–964	$2BaCO_3 \rightarrow 2BaO + 2CO_2$ $(1/4)Y_2O_3 + BaO + (3/2)CuO \rightarrow (1/2)YBa_2Cu_3O_{6.5}$ $(1/4)Gd_2O_3 + BaO + (3/2)CuO \rightarrow (1/2)GdBa_2Cu_3O_{6.5}$ $(1/2)YBa_2Cu_3O_{7-\delta} + (1/2)GdBa_2Cu_3O_{6.5} \rightarrow Y_{0.5}Gd_{0.5}Ba_2Cu_3O_{6.5}$

Table 2
Chemical reactions involved in the formation of $Y_{0.5}Nd_{0.5}Ba_2Cu_3O_{7-\delta}$.

Drop	Weight loss (Δm) (mg)	Δm (experimental) (%)	Δm (theory) (%)	Temperature range (°C)	Reaction
1–2	2.63	16.73	16.73	34–232	Water loss from the sample
3	2.91	18.51	20.01	232–316	$3Cu(C_2O_4) + (3/2)O_2 \rightarrow 3CuCO_3 + 3CO_2$ $3CuCO_3 \rightarrow 3CuO + 3CO_2$ $(1/4)Y_2(C_2O_4)_3 + (3/8)O_2 \rightarrow (1/4)Y_2(CO_3)_3 + (3/4)CO_2$ $(1/4)Nd_2(C_2O_4)_3 + (3/8)O_2 \rightarrow (1/4)Gd_2(CO_3) + (3/4)CO_2$
4	1.54	9.77	9.46	330–531	$2Ba(C_2O4) + O_2 \rightarrow 2BaCO3 + 2CO_2$ $(1/4)Y_2(CO_3)3 \rightarrow (1/4)Y_2O_3 + (3/4)CO_2$ $(1/4)Nd_2(CO3)3 + (1/4)CuO + (3/8)O_2 \rightarrow (1/4)Nd_2CuO4 + (3/4)CO_2$
5	0.86	5.44	6.83	738–973	$BaCO_3 \rightarrow BaO + CO_2$ $(1/4)Y_2O_3 + BaO + (3/2)CuO \rightarrow (1/2)YBa_2Cu_3O_{6.5}$ $(1/4)Nd_2Cu\ O_4 + Ba\ CO_3 + (5/4)CuO \rightarrow (1/2)NdBa_2Cu_3O_{6.5} + CO_2$ $(1/2)YBa_2Cu_3O_{6.5} + (1/2)NdBa_2Cu_3O_{6.5} \rightarrow Y_{0.5}Nd_{0.5}Ba_2Cu_3O_{6.5}$

Table 3
Chemical reactions involved in the formation of $Nd_{0.5}Gd_{0.5}Ba_2Cu_3O_{7-\delta}$.

Drop	Weight loss (Δm) (mg)	Δm (experimental) (%)	Δm (theory) (%)	Temperature range (°C)	Reaction
1–2	2.79	17.95	17.95	35–239	Water loss from the sample
3	2.70	17.44	19.50	239–316	$3Cu(C_2O_4) + (3/2)O_2 \rightarrow 3CuCO_3 + 3CO_2$ $3CuCO_3 \rightarrow 3CuO + 3CO_2$ $(1/4)Nd_2(C_2O_4)_3 + (3/8)O_2 \rightarrow (1/4)Nd_2(CO_3)_3 + (3/4)CO_2$ $(1/4)Gd_2(C_2O_4)_3 + (3/8)O_2 \rightarrow (1/4)Gd_2(CO_3)_3 + (3/4)CO_2$
4	1.40	9.01	9.22	316–501	$2Ba(C_2O_4) + O_2 \rightarrow 2BaCO_3 + 2CO_2$ $(1/4)Gd_2(CO3)3 + (3/8)O_2 \rightarrow (1/4)Gd_2O_3 + 0.5CO_2$ $(1/4)Nd_2(CO_3)_3 + (1/4)CuO + (3/8)O_2 \rightarrow (1/4)Nd_2CuO_4 + (3/4)CO_2$
5	0.82	5.26	6.65	753–955	$BaCO_3 \rightarrow BaO + CO_2$ $(1/4)Gd_2O_3 + BaO + (3/2)CuO \rightarrow (1/2)GdBa_2Cu_3O_{6.5}$ $(1/4)Nd_2Cu\ O_4 + BaCO_3 + (5/4)CuO \rightarrow (1/2)NdBa_2Cu_3O_{6.5} + CO_2$ $(1/2)GdBa_2Cu_3O_{6.5} + (1/2)NdBa_2Cu_3O_{6.5} \rightarrow Nd_{0.5}Gd_{0.5}Ba_2Cu_3O_{6.5}$

3.4. Electrical resistivity measurements

Electrical resistances of the prepared samples were measured as a function of temperature (Fig. 6). All samples possess single step feature, which indicates good grain connectivity within their structures [2]. The recorded zero resistance temperature ($T_{C(R=0)}$ and $T_{C(onset)}$) for YNdBCO, YGdBCO and NdGdBCO samples are (87 K, 95 K), (88 K, 92 K) and (90 K, 98 K) respectively as shown in Table 5. The mixed rare earth 123 phase superconductors do not show any

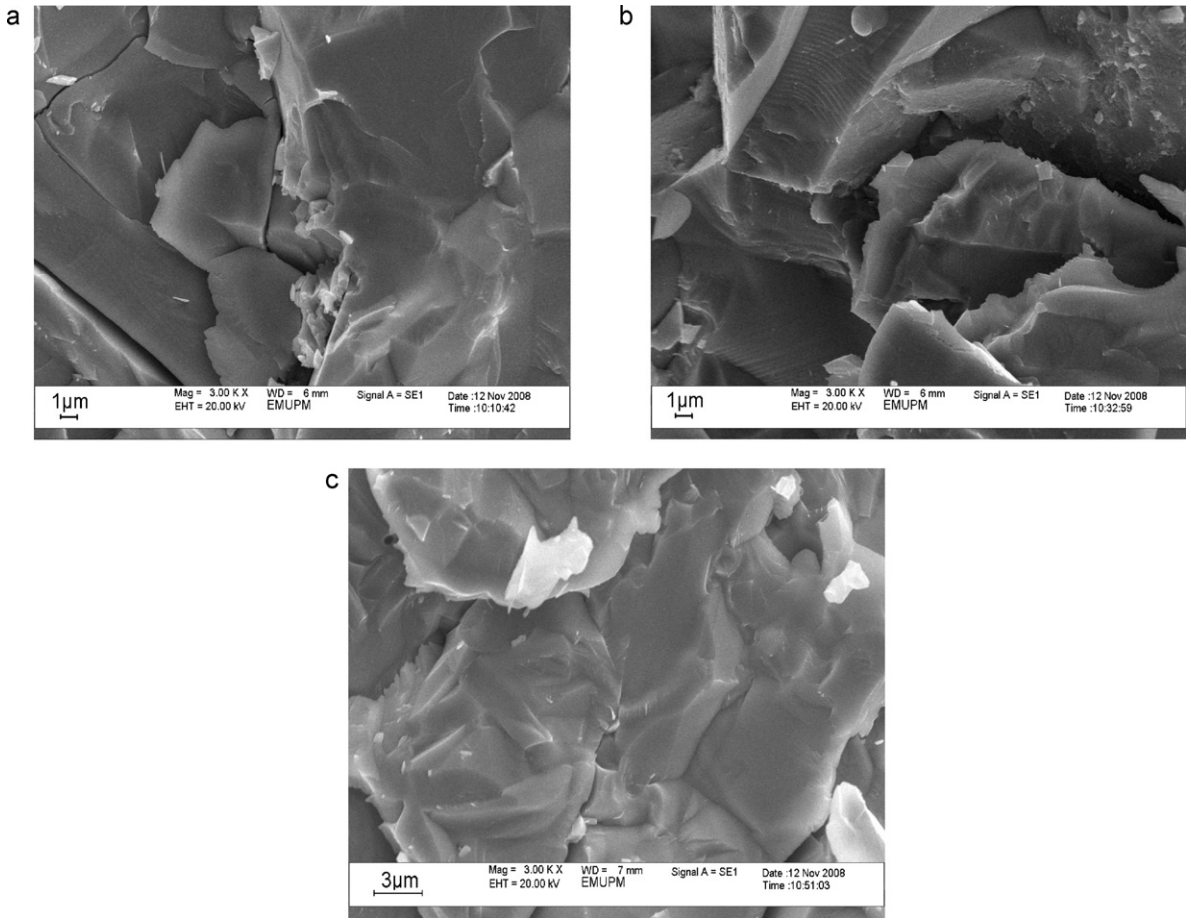

Fig. 7. SEM images of sintered (a)YGdBCO, (b)YNdBCO and (c)NdGdBCO samples.

significant improvement on their T_C. However, this gives a good indication that there is a possibility to have superconducting materials in their subsolidus systems.

3.5. Surface morphological study

The surface morphology of the samples sintered at 970 °C is shown in Fig. 7. The samples are highly compact with hardly noticeable pores within the structure. A dense and pore free structure is a prerequisite for low electric loss as the pores may be hygroscopic which may result in an increase in loss, particularly if soluble ions are leached from the solid phase.

Table 4
XRF analysis of YGdBCO sintered at 970 °C/15 h.

Sample	Analyte	Determined value		Theoretical value
		Wt%	Molar ratio	Molar ratio
YGdBCO	Y	9.36	0.62	0.50
	Gd	11.00	0.41	0.50
	Ba	48.56	2.08	2.00
	Cu	31.08	2.88	3.00

Table 5
The critical temperature of $REBa_2Cu_3O_{7-\delta}$ (RE: $Y_{0.5}Gd_{0.5}$, $Y_{0.5}Nd_{0.5}$, $Nd_{0.5}Gd_{0.5}$).

Sample	$T_{C(onset)}$ (K)	$T_{C(R=zero)}$ (K)
$Y_{0.5}Gd_{0.5}Ba_2Cu_3O_{7-\delta}$	92	87
$Y_{0.5}Nd_{0.5}Ba_2Cu_3O_{7-\delta}$	95	86
$Nd_{0.5}Gd_{0.5}Ba_2Cu_3O_{7-\delta}$	98	90

4. Conclusion

$REBa_2Cu_3O_{7-\delta}$ (RE: $Y_{0.5}Gd_{0.5}$, $Y_{0.5}Nd_{0.5}$, $Nd_{0.5}Gd_{0.5}$) metal oxalate precursors were successfully synthesised via co-precipitation method. BET analysis and TEM revealed that powders prepared via COP had relatively large surface area and ultrafine. Thermal analyses via TGA and DTA show identical thermal decomposition behaviour for samples, which underwent different chemical processes during their formation. Nd, unlike Y and Gd, reacted with copper oxide to form neodymium–copper binary compounds as observed in XRD after firing at 600 °C. This could be explained by the low activation barrier between neodymium and copper oxide that allowed the reaction to occur at lower temperature. Elemental analyses via XRF showed that the prepared compositions were in good agreement between their experimental and theoretical values. The zero resistance temperature ($T_{C(R=0)}$ and $T_{C(onset)}$) of samples were found to be at (87 K, 95 K), (88 K, 92 K) and (90 K, 98 K) for YNdBCO, YGdBCO and NdGdBCO samples, respectively. SEM images showed that the prepared samples had high dense structures with less pores.

Acknowledgements

This work was supported by the Ministry of Science, Technology and Innovation (MOSTI) grant no.: 03-01-04-SF0030. The authors would also like to thank the valuable support and discussions by all members of Material Chemistry Laboratory of Universiti Putra Malaysia.

References

[1] L.M. Yeoh, M. Ahmad, Characterization and synthesis of $Y_{0.9}Ca_{0.1}Ba_{1.8}Sr_{0.2}Cu_3O_{7-\delta}$ via combining sol–gel and solid-state route, J. Non-Cryst. Solids 354 (2008) 4012–4018.

[2] I. Hamadneh, A.M. Rosli, R. Abd-Shukor, N.R.M. Suib, S.Y. Yahya, Superconductivity of $REBa_2Cu_3O_{7-d}$ (RE = Dy, Y, Er, Ho) ceramics synthesized via coprecipitation method, J. Phys.: Conf. Ser. 97 (2008) 1.

[3] L.M. Yeoh, R. Abd-Shukor, The study on various wet chemistry techniques on $YBa_2Cu_3O_{7-d}$ superconducting oxides powder preparation, J. Non-Cryst. Solids 354 (2008) 4043–4048.

[4] I. Hamadneh, A.M. Ahmad, M.H. Wahid, Z. Zainal, R. Abd-Shukor, Effect of nano sized oxalate precursor on the formation of $GdBa_2Cu_3O_{7-d}$ phase via coprecipitation method, Mod. Phys. Lett. B 23 (16) (2009) 2063–2068.

[5] S.V. Kozlov, V.V. Pankov, The characterisation of $YBa_2Cu_3O_{7-\delta}$ layers produced by the diffusion couple technique, Czech. J. Phys. 46 (3) (1996) 1507–1508.

[6] J.G. Bednorz, K.A. Müller, Possible high T_c superconductivity in the Ba–La–Cu–O system, Z. Phys. B: Condens. Matter 64 (1986) 189–193.

[7] M.K. Wu, J.R. Ashburn, C.J. Torng, P.H. Hor, R.L. Meng, L. Gao, Z.J. Huang, Y.Q. Wang, C.W. Chu, Superconductivity at 93 K in a new mixed-phase Y–Ba–Cu–O compound system at ambient pressure, Phys. Rev. Lett. 58 (1987) 908–910.

[8] L. Sun, W. Li, S. Liu, T. Mertelj, X. Yao, Growth of a high performance SmBCO bulk superconductor with the addition of a $Sm_2Ba_4Cu_2O_9$ phase, Supercond. Sci. Technol. 22 (2009) 125008, 6 pp.

[9] H. Fujimoto, Developing a high-temperature superconducting bulk magnet for the Maglev Train of the future, JOM 50 (10) (1998) 16–18.

[10] K. Schlesier, H. Huhtinen, P. Paturi, Reduced intrinsic and strengthened columnar pinning of undoped and 4 wt% $BaZrO_3$-doped $GdBa_2Cu_3O_{7-\delta}$ thin films: a comparative resistivity study near T_c, Supercond. Sci. Technol. 23 (2010) 055010, 7 pp.

[11] S.I. Yoo, N. Sakai, H. Takaichi, T. Higuchi, M. Murakami, Melt processing for obtaining $NdBa_2Cu_3O_y$ superconductors with high T_c and large J_c, J. Appl. Phys. Lett. 65 (5) (1994) 633–635.

[12] Y. Shiohara, M. Nakamura, T. Hirayama, Y. Ikuhara, Single crystal growth of Nd123 superconductive oxides: new process to control critical currents, J. Kor. Phys. Soc. 31 (1) (1997) 56–59.

[13] F. Giovannelli, J. Noudem, D. Brouri, D. Bourgault, I. Monot-Laffez, Synthesis and transport properties of oxygen controlled melt growth textured (MixedRE)$Ba_2Cu_3O_y$ (RE = Nd, Sm, Gd, Eu), Supercond. Sci. Technol. 18 (2005) S149–S152.

[14] M. Muralidhar, H.S. Chauhan, T. Saitoh, K. Segawa, K. Kamada, M. Murakami, Application of oxygen controlled melt growth (OCMG) in ternary RE123 systems, Phys. C. 280 (1997) 200–204.

[15] M. Muralidhar, M.R. Koblischka, M. Murakami, Improvement of critical current densities in bulk superconductors of the 123-type, Phys. Status Solidi A (1999) R7–R8.

[16] M. Muralidhar, H.S. Chauhan, T. Saitoh, K. Kamada, K. Segawa, M. Murakami, Effect of mixing three rare-earth elements on the superconducting properties of $REBa_2Cu_3O_y$, Supercond. Sci. Technol. 10 (1997) 663–670.

[17] G.E. Shter, G.S. Grader, YBCO oxalate coprecipitation in alcoholic solutions, J. Am. Ceram. Soc. 77 (1994) 1436–1440.

[18] G.R. Paz-Pujalt, A.K. Mehrotra, S.A. Ferranti, J.A. Agostinelli, Solid state reactions in the formation of $YBa_2Cu_3O_{7-\delta}$ high T_c superconductor powders, Solid State Ionics 32–33 (1989) 1179–1182.

[19] G.S. Grader, P. Yossefov, G.M. Reisner, G.E. Shter, Synthesis of Nd123 superconducting powder via oxalate coprecipitation, Phys. C 290 (1997) 70–88.